Investigation of High Penetration and Dispersion of Functional Nanoparticles in Leather

by

Ji-bo Zhou,[1] Nan Sun,[1] Xue-pin Liao[1,2]* and Bi Shi[1,2]

[1]*Department of Biomass and Leather Engineering, Sichuan University,* Chengdu 610065

[2]*National Engineering Research Center of Clean Technology in Leather Industry,* Chengdu 610065

Abstract

The use of nanoparticle-based functional leather products has stimulated sustainable growth of the conventional leather industry. However, functional nanoparticles (FNPs) face challenges to be well penetrated and dispersed in leather because of their aggregation and mismatch charges with leather. In this study, the acrylic resin (AR) retanning agent, which was originally utilized in leather processing, was applied for the modification of FNPs. It has been demonstrated that AR can improve the electrostatic and steric repulsion among nanoparticles, inhibiting their aggregation and ensuring their penetration and dispersion in leather. Because of the limitation of leather porosity, the maximum loading amount for FNPs was about 40wt% (based on leather weight). The leather got higher results in fullness, thickening ratio, and tensile strength when the loading amount of FNPs was 11.25%. Moreover, the proposed approach in this study can be used well for other types of FNPs loaded in leather, suggesting its broad applicability.

Introduction

With the incorporation of functional nanoparticles (FNPs), conventional leather has recently demonstrated great potential in various high-end applications such as ultraviolet blocking, electromagnetic shielding, and *X*-ray shielding.[1-2] The development of these functional leather materials not only increases the value-added of natural leather but also promotes sustainable growth of the conventional leather industry.[3] However, there are also troublesome issues that must be resolved in this process. For example, the effective penetration and dispersion of FNPs into leather is a prerequisite for fabricating advanced functional leather, but FNPs tend to congregate as a result of their heightened van der Waals attractive forces (Figure 1a). The agglomerated FNPs exhibit very large size, and therefore hindering their penetration in leather.[4] Moreover, there are many surface charges present on nanoparticles. As leather making is a well-known charge-related process,[5] the mismatch of surface charges between FNPs and leather further inhibits their penetration and dispersion process.

There are primarily two methods to prevent the agglomeration of FNPs: electrostatic modification and steric repulsion (Figures 1b and 1c).[6] Electrostatic modification involves the adsorption of charged stabilizer molecules on the surface of FNPs, which creates an electrical double layer that facilitates the electrostatic repulsion, thereby restraining aggregation and adjusts the charge on the surface of FNPs.[7] Steric repulsion involves using polymers to increase the steric repulsion among FNPs, thereby inhibiting the aggregation of FNPs.[8] Currently, the steric repulsion method is mainly achieved by surfactants comprising a hydrophilic head group and a hydrocarbon chain (hydrophobic group).[9] The hydrophobic segments of surfactants form a physical barrier on the surface of NPs via hydrophobic interactions, while hydrophilic segments increase the stability of FNPs in suspensions such as water and ethyl alcohol. Based on the above two methods, several chemicals such as polyionic liquids, chitosan, hydrogenated castor oil, and polyethylene glycol have all been attempted as modifications to facilitate the penetration and dispersion of FNPs in leather.[10-13] These agents are effective in specific conditions, but they usually suffer a long time of reaction, multiple steps, cost-prohibitive and the use of more hazardous chemical agents.[14] Besides, the introduction of these chemicals may reduce the comprehensive performances of leather, such as wearing comfort and mechanical strength. Therefore, there is a great demand to develop a novel approach to realize the effective penetration and dispersion of FNPs in the leather.

Looking across the leather-making process, acrylic resin (AR) used in the leather retanning process may offer a solution to the FNPs aggregation issue. In general, AR is a polymer synthesized through the free radical co-polymerization of vinyl monomers, and it has been widely used as a retanning agent in the leather industry due to its excellent filling property.[15] To achieve a better filling performance, AR used in the leather retanning process is usually composed of monomers with hydrophilic groups (-COOH, $-NH_2$) and hydrophobic groups (long-chain acrylates), endowing it the capacity to stabilize FNPs via steric stabilization. Furthermore, AR typically shows negative charges because of the presence of abundant carboxyl groups in its structure, which may increase the

*Corresponding author email: xpliao@scu.edu.cn

Manuscript received March 30, 3023, accepted for publication May 7, 2023.

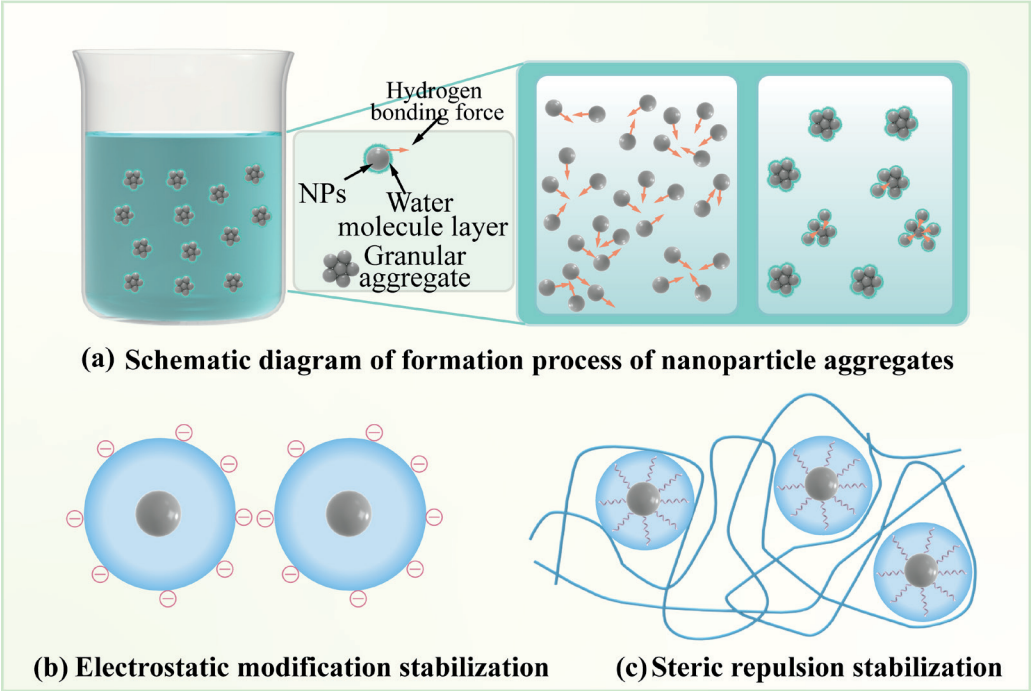

Figure 1. **(a)** Schematic of the aggregation of FNPs. FNPs stabilized by electrostatic modification **(b)** and steric repulsion **(c)**.

electrostatic repulsion between FNPs and inhibit their aggregation. By the synergistic of steric stabilization and electrostatic modification, it is believed that AR would effectively promote the penetration and dispersion of FNPs in leather. Moreover, as AR is a commonly used agent in leather processing, there are no concerns over increased costs and decreased performance of leather. To our knowledge, no studies have yet investigated the effects of AR on the penetration and dispersion of FNPs in leather.

In this study, a novel approach was developed to realize the good penetration and dispersion of FNPs in leather using AR as a modifier. Specifically, gadolinium oxide (Gd_2O_3) nanoparticles (generally used as a functional component of neutron absorption and attenuation of *X*-rays) were considered as representative and the surface morphology of modified Gd_2O_3 FNPs as well as their dispersity and charge properties in water were completely characterized to clarify their penetration and dispersion mechanism in leather. Beyond that, the influence of FNPs on the performance of functional leather was also presented. In addition, the FNPs of B_4C and Bi_2O_3 were also tested to verify the universality of this approach.

Materials and Methods

Materials

Gd_2O_3, B_4C, and Bi_2O_3 nanoparticles (99.9%, 500 nm) used in this study were all obtained from Guangzhou Nano Chemical Technology Co., Ltd. The chrome-tanned and vegetable-tanned leather (both shaved to 1.2 mm) were provided by the National Engineering Laboratory for Clean Technology of Leather Manufacture at Sichuan University. A commercial AR (copolymerized by acrylic acid and long-chain vinyl ester monomers, about 33 wt%) was purchased from Sichuan Decision New Material Technology Co., Ltd. (China). All other chemicals were of analytical grade and purchased from Chengdu Kelong Chemical Co., Ltd.

Modification of FNPs

First, AR was dissolved in water to form a 1:1 (w/w) solution, then Gd_2O_3 FNPs were added to the solution and dispersed by ultrasonication for 30 min at room temperature, and the suspension was stirred at 80°C for 2 h to complete the modification. Finally, the modified Gd_2O_3 was collected and dried in a vacuum at 80°C for 2 h before being used. B_4C and Bi_2O_3 nanoparticles were similarly modified using the same manner.

Physicochemical properties of modified FNPs

FTIR spectra of the pristine and modified Gd_2O_3 nanoparticles were recorded using a Fourier transform infrared spectrometer (Nicolet IS10, Thermo Scientific, USA). X-ray photoelectron spectroscopy (XPS) measurements were conducted using an Escalab Xi+ (Thermo Fisher, USA).

To evaluate the dispersibility and stability of the pristine and modified Gd_2O_3 nanoparticles, they were separately dispersed in deionized water at 0.4 mg/mL and left undisturbed at room temperature for

different times to obtain Gd_2O_3 fluids. The absorbance of FNPs fluids was determined using a spectrophotometer (PerkinElmer, Japan). The size and zeta potential of pristine and modified Gd_2O_3 nanoparticles (in water) were tested using NanoBrook Omni (Brookhaven, USA).

To observe the dispersion of FNPs in the leather matrix, SEM (Nova NanoSEM450, FEI, USA) was used to capture the cross-section of the composites. The composition analysis was performed using energy-dispersive X-ray spectroscopy (EDS, Azteclive Ultim Max 100, Oxford Instruments, UK). The loading amounts of FNPs were determined through ICP-OES after digestion.

Penetration of modified FNPs in leather

Modified FNPs were introduced into the leather matrix using a typical retanning process summarized in Table I.

Effect of different factors on the penetration of FNPs in leather

The effect of different factors on the loading amounts of FNPs, including the amounts of FNPs, pH of bath solution, and water washing, were completely investigated. In particular, to assess the changes of FNPs amount in the leather matrix over pH, the pH of the bath solution was adjusted using different amounts of sodium bicarbonate and formic acid after retanning by modified FNPs via the process shown in Table I, and the leather samples were then treated in the bath for another 2 h before fatliquoring. Furthermore, the water-washing resistance of samples before and after fatliquoring was assessed, with each water-washing cycle of 1 h.

Influence of FNPs on the mechanical performance of leather

All samples were maintained at a temperature of 25° ± 2°C and a relative humidity of 65% ± 2% for over 48 h before measuring. Using a dial thickness gauge (MingYu, China), the average thickness of leather samples was measured, and the thickening ratio (R) was calculated using the formula:

$$R = \frac{(S_2 - S_1)}{S_1} \times 100\%$$

where S_1 and S_2 are the average thicknesses of leather samples before and after retanning with FNPs, respectively.

The physical and mechanical properties of samples, such as tensile strength, and tearing strength, were evaluated using an ISO 3377-2:2016 and ISO 3376:2020 compliant universal testing machine (GOTECH, China). The micropore structures of composites were analyzed using a mercury intrusion porosimeter (Micromeritics, USA).

Table I
Retanning Processes

Process	Chemicals	Dosage %	Temperature (%)	Duration (min)	Remarks
Rewetting	Water	250	40		
	Degreasing agent	0.3			
	Formic acid	0.5		60	pH≈3.2, Drain
Washing	Water	400		10	Drain
Neutralization	Water	200	35		
	Sodium formate	2		30	
	Neutralization tannins	2			
	Sodium bicarbonate	1		60	pH≈5.5, Drain
Washing	Water	400		10×2	Drain
Retanning	Water	100	35		
	FNPs	10/20/30/40/60		90	
Fatliquoring	Water	100	50		
	SO	8		50	
	Formic acid	2		4×15	pH≈3.4
Washing	Water	400		10×3	Drain
Note: based on wet blue weight (w/w)					

Results and Discussion

Basic properties of modified FNPs

Figure 2a shows the modification process of Gd_2O_3 FNPs by AR. AR, a commonly used polymer in the leather retanning process, has numerous hydrophobic bonds that facilitate its combination with Gd_2O_3 FNPs via hydrophobic interactions.[16] After modification, a physical barrier was generated on the surface of FNPs, exposing the hydrophilic groups of AR to aqueous environment, as well as leads to additional stabilization via short-range repulsive hydration forces and enhances their steric stabilization. Furthermore, the electronegative carboxyl groups in the molecule of AR can promote electrostatic repulsion among nanoparticles, further enhancing their dispersion stabilities.

To determine the surface structure of the modified Gd_2O_3 FNPs, FTIR analysis was conducted and is shown in Figure 2b. The characteristic peak at 543 cm^{-1} in the spectra of pristine Gd_2O_3 FNPs corresponded to the vibration absorption of the Gd–O–Gd bonds in Gd_2O_3.[17] The broad absorption peak observed at 3463 cm^{-1} corresponded to the O–H absorption band, and it was attributed to the stretching vibration of adsorbed water molecules on the surface of Gd_2O_3.[18] Owing to the atmospheric water and CO_2 molecules, two peaks at 1389 and 1500 cm^{-1} were observed, and they correspond to O–H and C–O stretching, respectively.[19] For the modified Gd_2O_3, a new peak at 1557 cm^{-1} was observed, which is also seen in the AR spectra. This peak was assigned to the vibration of -COOH, indicating the successful adherence of -COOH onto the surface of Gd_2O_3.[20] The new peaks detected at 2948 and 1416 cm^{-1}, which were attributed to $-CH_2-$ in the long chains of AR, further enhanced the modification.[21] AR contains long hydrophobic tails, and the hydrophobic interaction between AR and Gd_2O_3 allows the hydrophobic tails to drain onto the cluster surface, which facilitates the adsorption of AR molecules on the surface of Gd_2O_3 nanoparticles.

The modification process of Gd_2O_3 FNPs can then be confirmed by XPS analysis. As shown in Figure 2c, the XPS survey spectra of pristine Gd_2O_3 primarily demonstrate two distinct peaks at 142.82 and 531.25 eV, which correspond to Gd 4d and O1s, respectively.[22] However, after modification by AR, the relative intensity of Gd 4d considerably decreased, while C1s increased, indicating successful adherence of AR on the surface of Gd_2O_3 nanoparticles. This conclusion is supported by the proportion of each element revealed by XPS (Figure 2d), which shows a decrease in the fraction of the Gd element from 14.77% to 1.80% and an increase in C from 19.47% to 66.33% after modification. Furthermore, Figure 2e shows that the O 1s curves of pristine Gd_2O_3 could be fitted into two peaks at 531.24 and 528.61 eV, assigned to the Gd–O and O–H bonds, respectively.[23]

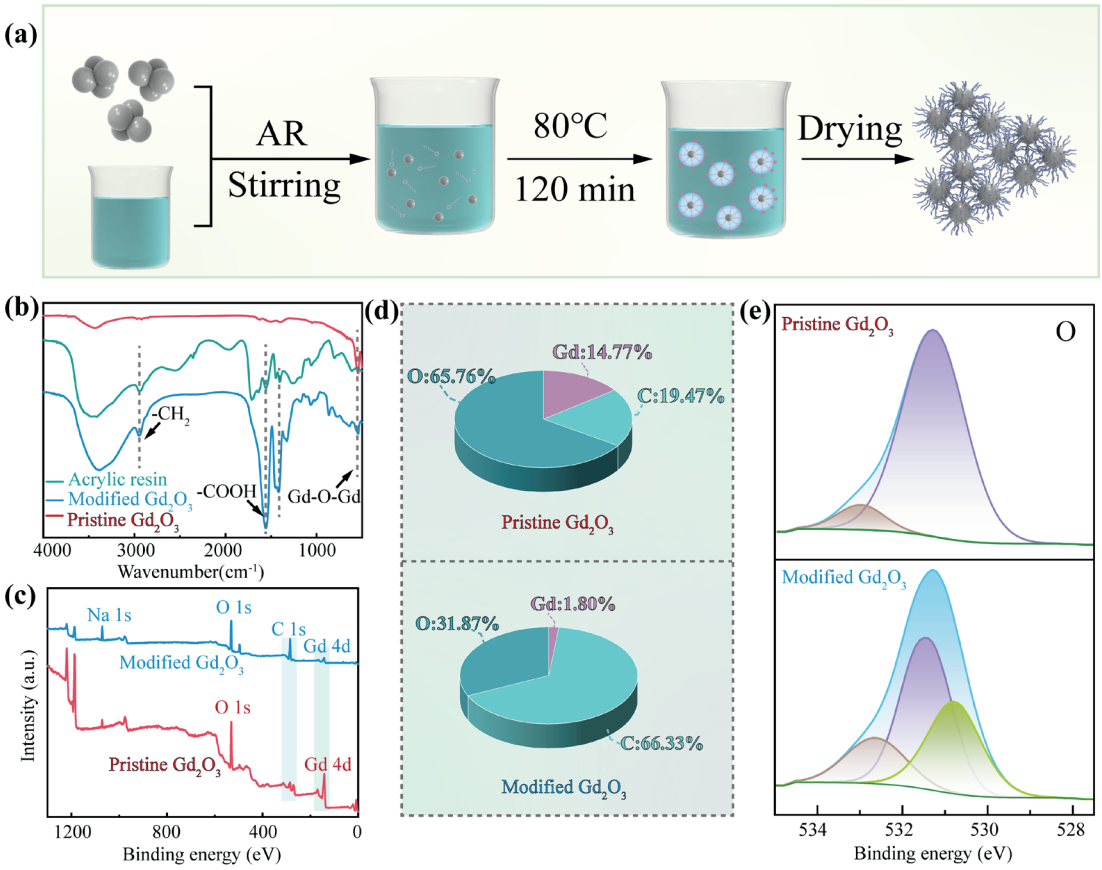

Figure 2. **(a)** Modification process of Gd_2O_3 FNPs by AR, **(b)** FTIR of pristine and modified Gd_2O_3 FNPs, **(c)** High-resolution XPS spectrum of the full spectrum, **(d)** Proportion of elements, and **(e)** O 1s revealed by XPS.

After being modified by AR, a new peak assigned to C=O, can be observed at 530.78 eV; this peak was raised from AR, further confirming the success of the modification.[24]

Analysis of the dispersibility of modified Gd_2O_3 FNPs in water

Leather-making processes are mostly applied in an aqueous environment, where FNPs are more prone to agglomerate because of surface forces such as Van der Waals and electrostatic forces, forming a secondary agglomeration structure that hinders the penetration of FNPs in the leather matrix.[25] Therefore, investigating the dispersion ability of FNPs in water is important to understand their penetration and dispersion process in leather.

In this study, the dispersion stabilities of pristine and modified Gd_2O_3 FNPs in water were examined using a settlement test. As shown in Figure 3a, pristine Gd_2O_3 FNPs were exceedingly unstable because of their large surface area and strong Van Der Waals interaction, resulting in rapid agglomeration and settling at the bottom of the bottle. However, the Gd_2O_3 FNPs modified with AR demonstrated considerably improved dispersion stability under the same condition. The long-chain vinyl ester in the AR molecule lies the foundation for the combination between AR and Gd_2O_3 FNPs via hydrophobic interaction, forming a physical barrier on the surface of FNPs and enhancing its steric stabilization. Furthermore, the charged carboxyl groups in AR can enhance the electrostatic repulsion between nanoparticles and inhibit their aggregation. The synergistic effect of steric stabilization and electrostatic modification largely enhanced the stability of FNPs in water.

According to the literature, only individual FNP exhibit characteristic bands in the UV-vis region, whereas agglomerated FNPs are inactive.[26] As shown in Figure 3b, pristine FNPs exhibit weak absorbance in the wavelength range from 200 nm to 800 nm, with absorbance decreasing as wavelength increases. However, after modification, the absorbance of modified Gd_2O_3 FNPs is higher than that of pristine FNPs, indicating the presence of a certain amount of individually dispersed Gd_2O_3 FNPs in dispersions. This finding is consistent with the settlement investigation, which further demonstrates that AR can effectively inhibit the aggregation of FNPs and improve their dispersibility in water.

The size and electrostatic properties of FNPs are crucial factors that affect their penetration and dispersion in NL. The particle size and zeta potential of the FNPs were therefore determined in this study, and the results are shown in Figures 3c-d. Pristine Gd_2O_3 FNPs (500 nm) exhibited agglomeration in water, resulting in a large particle size of 1632.22 nm, which may impede their penetration into leather The large particle size of FNPs may hinder their penetration in leather. However, after modification with AR, the particle size of modified FNPs decreased to 714.36 nm, showing the effectiveness of AR in preventing the FNPs agglomeration and facilitating their penetration and dispersion in leather. Furthermore, the zeta potential of modified Gd_2O_3 FNPs at different pH was mostly negative because of the increase of electrostatic repulsion caused by the introduction of abundant carboxy groups, remarkably lower than that of pristine Gd_2O_3 FNPs (Figure 3d).[27] As chrome-tanned leather is considered electropositive in the retanning process, the electrostatic attraction between modified Gd_2O_3 FNPs and leather can provide a driving force for the penetration of FNPs in leather. Furthermore, the carboxyl groups on the surface of modified Gd_2O_3 FNPs can coordinate with Cr^{3+}, which is favorable for combining Gd_2O_3 FNPs with leather.

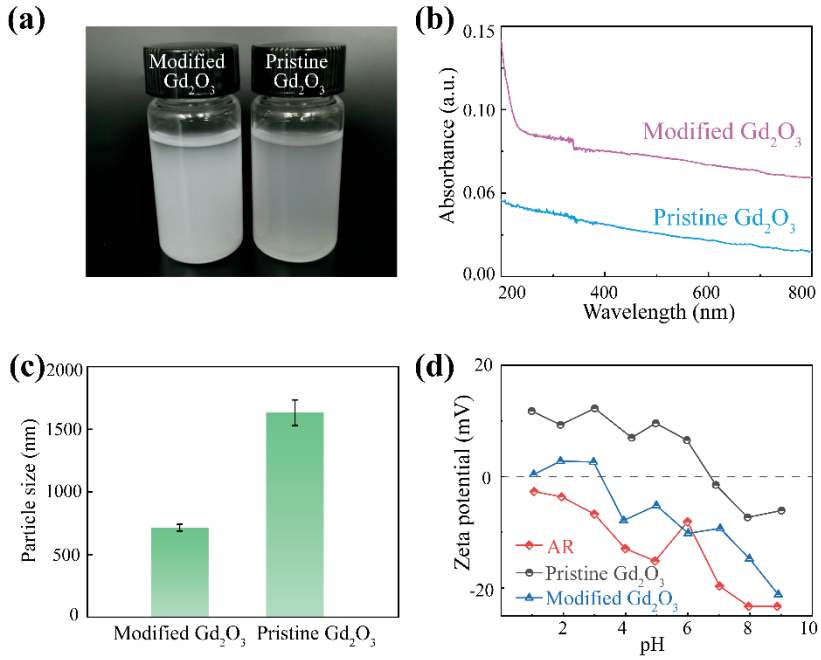

Figure 3. **(a)** Images of pristine and modified Gd_2O_3 FNPs in deionized water. UV-vis **(b)**, particle size **(c)**, and zeta potential **(d)** of pristine and modified Gd_2O_3 FNPs in deionized water.

The aforementioned results have confirmed the successful attachment of carboxyl groups on the surface of Gd_2O_3 FNPs, resulting in modified Gd_2O_3 FNPs with electronegative properties and smaller particle size in water due to their electrostatic and steric repulsion. On the one hand, AR modification improves the electrostatic and steric repulsion among nanoparticles, inhibits the formation of large agglomerations, and ensures the penetration of Gd_2O_3 FNPs in leather. On the other hand, the modified Gd_2O_3 FNPs reveal strong electrostatic interactions with the electropositive leather, which undoubtedly provide a powerful driving force for their penetration into leather.

Penetration of pristine/modified FNPs in leather

To investigate the penetration of modified Gd_2O_3 FNPs in leather, cross-sectional SEM observation of retanned leather were conducted. As shown in Figure 4a, due to the large average particle size resulting from agglomeration and the charge mismatch between FNPs and leather, pristine FNPs struggled to penetrate leather, leading to significant non-uniformity of Gd elements near the grain layer. However, after modification with AR, uniform dispersion of Gd elements was observed (Figure 4b), indicating the successful penetration of modified FNPs in the leather.

Figure 4c summarizes the penetration of pristine and modified Gd_2O_3 FNPs in leather. Commonly, leather making is the penetration and combination of chemical substances in leather, and these two processes are fully affected by the particle size and surface charge of chemicals. On the one hand, AR can effectively form physical barriers on the surface of FNPs with its surface activity, inhibiting the aggregation of FNPs and favoring the penetration of FNPs. On the other hand, the charged groups within the structure of AR can tune the surface charge of FNPs, further enhancing their penetration and dispersion in leather. Overall, the combined effect of these factors facilitates the uniform penetration and dispersion of modified FNPs in leather.

Effect of different factors on the penetration and dispersion of modified FNPs in leather

To further understand the penetration and dispersion of FNPs in leather, various conditions were investigated with loading amounts of FNPs as the index. First, the variation of the loading amounts with the usage of FNPs is shown in Figure 5a. As shown, the loading amounts of FNPs were increased with the increasing dosage of FNPs and gradually attained a plateau. Structurally, leather possesses a sophisticated hierarchical structure from the nanoscale to the macroscale, and the space ranges from micrometers to millimeters among collagen fibers of leather laying solid foundations for the penetration of nanoparticles into the hierarchical network of leather.[28] Although chromed-tanned leather exhibit a high porosity, it is still limited.[29] So, the loading amount of FNPs is saturated as further increasing its dosage.

The effect of pH on FNPs loading amounts was investigated by adjusting the bath pH using formic acid and sodium bicarbonate. Figures 5b-c show that decreasing pH resulted in an increased loading amount of FNPs, indicating the significant influence of surface charge on the penetration of FNPs in leather. The electrostatic attraction between leather and negatively charged modified FNPs was improved when the electropositive property of chrome-tanned leather increased due to the decreased pH of

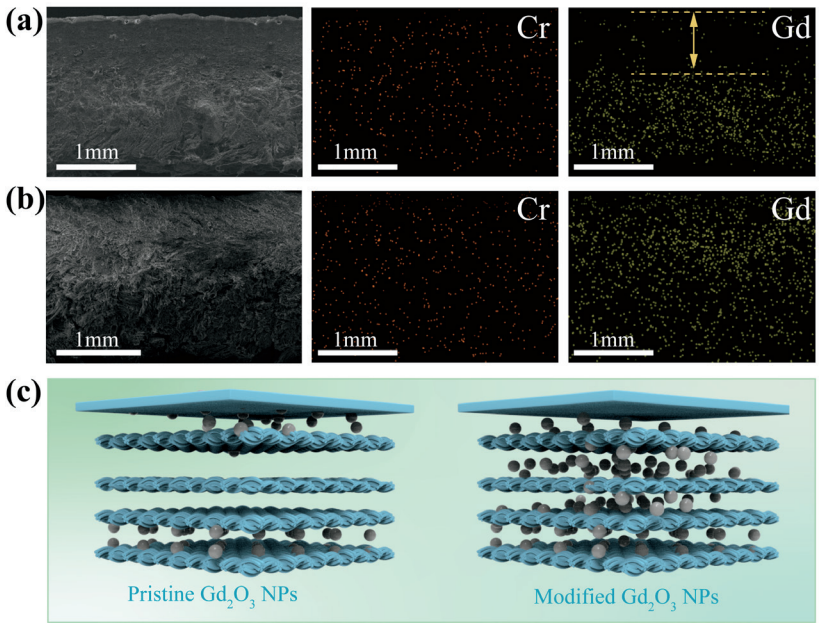

Figure 4. SEM observation of the cross-session of leather retanned with pristine **(a)** and modified **(b)** Gd_2O_3 FNPs. **(c)** Schematic diagram illustrates the penetration of pristine and modified Gd_2O_3 FNPs in leather.

the bath solution. By decreasing the pH of the bath solution, the electropositive property of chrome-tanned leather increased, and the electrostatic attraction between leather and negatively charged modified FNPs was improved.[30] Owing to the enhanced driving force, the penetration of FNPs in leather is much easier. On the contrary, the positive charge of leather was decreased by the increased pH, and the electrostatic attraction between leather and FNPs was weakened, resulting in the lower absorption of FNPs. This result shows that the penetration of FNPs in leather was substantially associated with surface charge, and AR modification can effectively improve the penetration and dispersion of FNPs in leather.

The binding force between FNPs and leather was assessed by investigating the water-washing resistance of prepared composites. Figure 5d shows that the loading amounts of Gd_2O_3 decreased with increased time of water washing cycles, indicating that the combination between FNPs and leather is not strong enough and can be broken by mechanical force. However, after fatliquoring, as the increased times of water washing cycles, the decreasing trend on the loading amounts of FNPs were significantly weakened and it only presented a reduction of 0.03% after three times of water washing. This phenomenon can be assigned to the reason that the fatliquoring process improved the hydrophobicity of the leather, enhancing the hydrophobic interaction between FNPs and leather, therefore enhancing their combination.[31]

Influence of modified FNPs on the organoleptic and physical performance of leather

The organoleptic properties and physical strength characteristics of composites play a key precondition in ensuring the wear comfort of functional leather. To comprehensively investigate the influence of FNPs on the organoleptic properties of leather, the porosity, fullness, thickening ratio, and mechanical performance of leather samples with different amounts of Gd_2O_3 FNPs were all investigated. From Figure 6a, the porosity of the blank leather sample was 64.75%. Because of the filling of Gd_2O_3 FNPs, the porosity of composites sharply decreased, and it was only 46.09% when the loading amounts of Gd_2O_3 FNPs was 39.64%.

The compression-resilience performances of composites are presented in Figure 6b-c. Generally, a higher compressed and resilient thickness implies a better fullness of leather. It can be seen that the leather sample got the best fullness performance when the loading amount of Gd_2O_3 FNPs was 11.25%, and it decreased with a further increase of Gd_2O_3 FNPs amounts, indicating that too high loads of FNPs may decrease the performance of leather. This conclusion can also be supported by the changes in thickening ratio (Figure 6d), where samples got higher results when the loading amount of Gd_2O_3 FNPs was 11.25% and 19.40%, while it decreased as the loading amount of Gd_2O_3 FNPs further increased. Moreover, because of the filling of Gd_2O_3 FNPs, the compressibility of composites all decreased (Figure 6e), but they are mostly more than 5.0 mm, which will not significantly influence their wearable performance. Besides, the density of leather improved obviously due

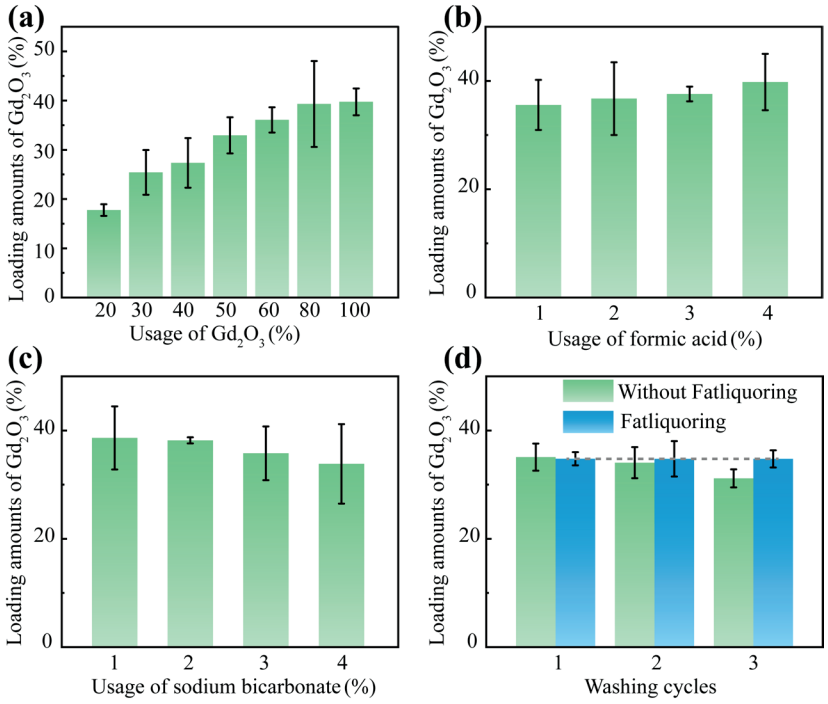

Figure 5. Influence of FNPs usage **(a)**, acid **(b)**, alkaline **(c)**, and washing **(d)** on the loading amounts of Gd_2O_3 FNPs.

to the introduction of Gd_2O_3 FNPs (Figure 6f). From Figures 6g-h, the tensile and tear strength of samples all exhibited a noticeable increase, possibly because of the interaction between FNPs and collagen fiber. More importantly, the shielding efficiency of composites for *X*-rays at 48.3 KeV was investigated when the usage of Gd_2O_3 FNPs was 20%, and the results were shown in Figure 6i. Due to the better penetration and dispersion of FNPs, the modified Gd_2O_3-leather composites get a higher performance, which was 37.94% higher than that of pristine Gd_2O_3-leather composites, demonstrating the necessity of modification in elevating the performance of functional leather.

To determine the universality of the proposed AR modification method, the penetration of B_4C FNPs (500 nm) in chrome-tanned leather and Bi_2O_3 nanoparticles (500 nm) in vegetable-tanned leather were also investigated. Because B_4C is dark black and Bi_2O_3 FNPs are yellow, their penetration in leather can be easily reflected by the color changes on the cross-sections of retanned leathers. As shown in Figure 7a and 7c, it can be observed that the color of cross-section of leather retanned by pristine B_4C/Bi_2O_3 was uneven, implying the difficulty of FNPs in penetration. After being modified by AR, FNPs are well dispersed in leather (Figures 7b and 7d), indicating that the AR modification method fits well with different FNPs.

Conclusion

In this study, a new method was developed for achieving effective penetration and dispersion of FNPs in leather. This was achieved by utilizing acrylic resin as a modifier, which enhances the electrostatic and steric repulsion among nanoparticles, therefore inhibiting their aggregation and ensuring their penetration and dispersion in

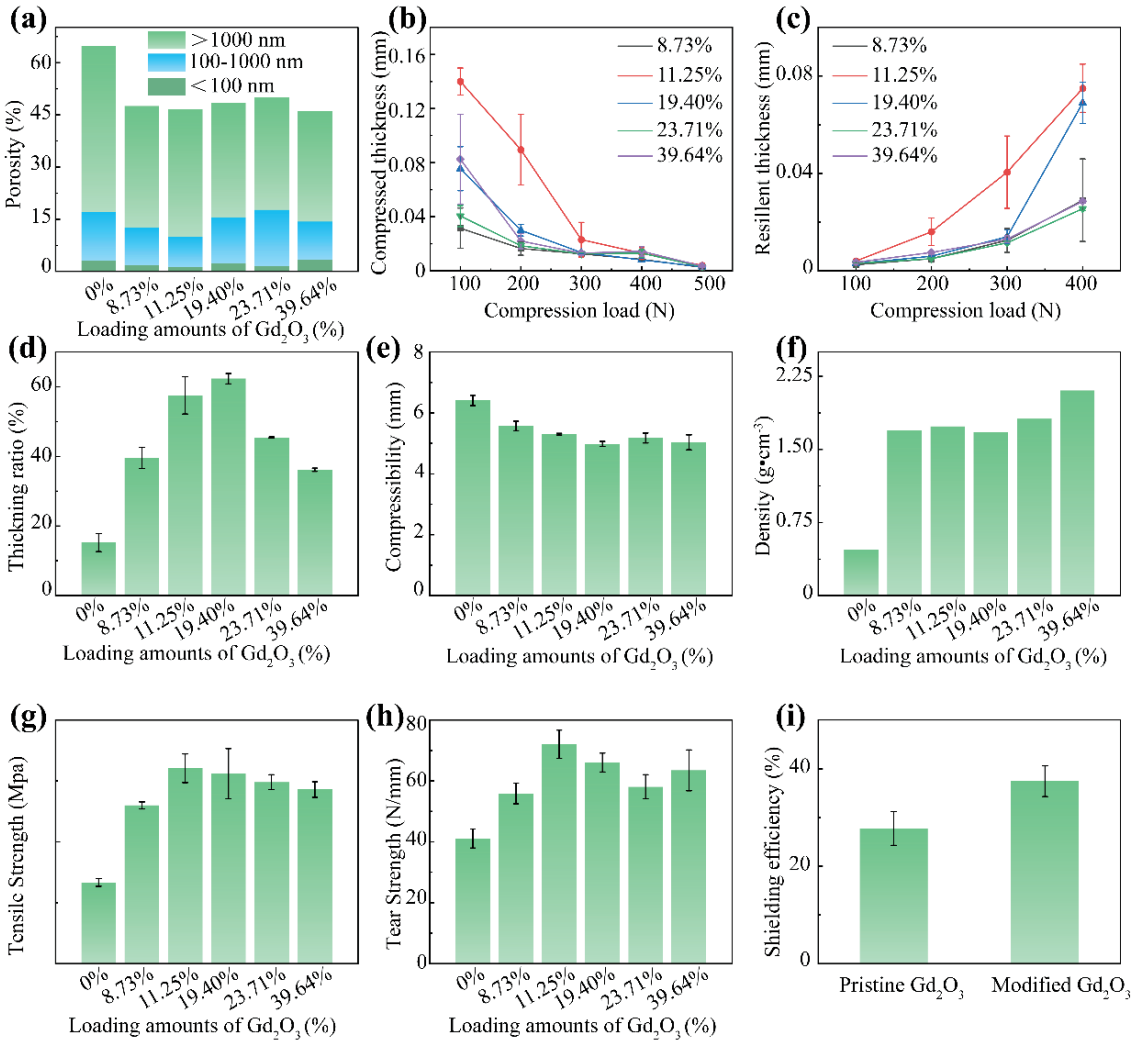

Figure 6. **(a)** Porosity, **(b)** compression, **(c)** resilience, **(d)** thickening ratio, **(e)** compressibility, **(f)** density, **(g)** tensile strength, **(h)** tear strength of different composites, and **(i)** *X*-rays shielding efficiency of different composites.

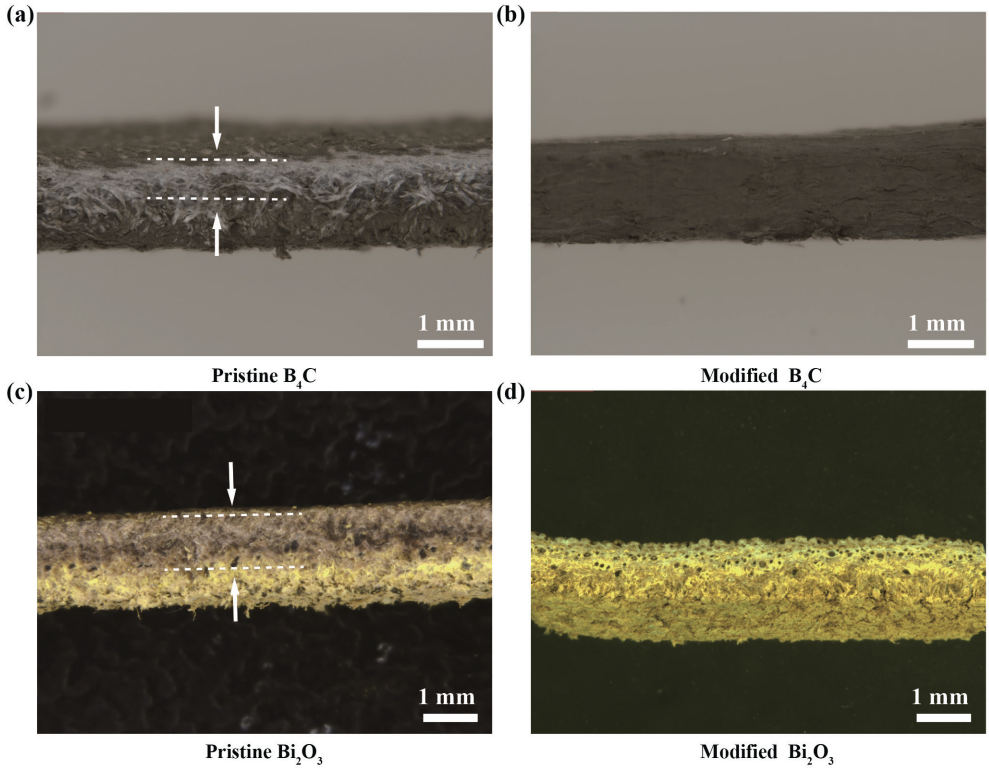

Figure 7. Microscopic pictures of the cross sections of chrome-tanned leather retanned with pristine **(a)** and modified **(b)** B_4C FNPs, and vegetable-tanned leather retanned with pristine **(c)** and modified **(d)** Bi_2O_3 FNPs.

leather. Furthermore, the increase in the leather's electropositivity and hydrophobicity can promote FNP penetration. However, too high loads of FNPs may decrease the performance of composites. The novel acrylic resin-modified approach presented in this study could be applied to other FNPs, offering a useful strategy for the production of nanoparticle-based functional leather.

Acknowledgment

This study was financially supported by the National Natural Foundation of China (22278279). We also thank Dr. Xiu He of the College of Biomass Science and Engineering, Sichuan University for experimental assistance.

Reference

1. Cosma, D. V., Tudoran, C., Coroș, M., et al.; Modification of cotton and leather surfaces using cold atmospheric pressure plasma and TiO_2-SiO_2-reduced graphene oxide nanopowders, *Materials* **16**, 1397, 2023.
2. Shen, Y., Zhou, J., Han, Z., et al.; Natural leather based gamma-ray shielding materials enabled by the coordination of well-dispersed Bi^{3+}/Ba^{2+} ions and RE_2O_3 coating, *Journal of Leather Science and Engineering* **4**, 15, 2022.
3. Zhu, J., Li, Z., Zou, Y., et al.; Advanced application of collagen-based biomaterials in tissue repair and restoration, *Journal of Leather Science and Engineering* **4**, 30, 2022.
4. Yu, S., Liu, H., Yang, R., et al.; Aggregation and stability of selenium nanoparticles: Complex roles of surface coating, electrolytes and natural organic matter, *Journal of Environmental Sciences* **130**, 14-23, 2023.
5. Wang, Y. N., Hu, L. Y.; Essential role of isoelectric point of skin/leather in leather processing, *Journal of Leather Science and Engineering* **4**, 25, 2022.
6. Guerrini, L., Alvarez-Puebla, R. A. and Pazos-Perez, N.; Surface modifications of nanoparticles for stability in biological fluids, *Materials* **11**, 1154, 2018.
7. Xu, Y., Fourniols, T., Labrak, Y., et al.; Surface modification of lipid-based nanoparticles, *ACS Nano* **16**, 7168-7196, 2022.
8. Hatchell, D., Song, W. and Daigle, H.; Effect of interparticle forces on the stability and droplet diameter of Pickering emulsions stabilized by PEG-coated silica nanoparticles, *Journal of Colloid and Interface Science* **626**, 824-835, 2022.
9. Wang, B., Zhong, X., Zhang, Y., et al.; Microspheres assembled by WO_{3-x} nanoparticles under action of dual surfactants: Structure and photoluminescence properties, *Optical Materials* **129**, 112550, 2022.
10. Zhao, P., Gao, D., Lyu, B., et al.; Fabrication of effective electromagnetic shielding leather with a chromium-free multi-network structure, *Journal of Cleaner Production* **374**, 133856, 2022.

11. Freitas, D. S., Teixeira, P., Pinheiro, I. B., et al.; Chitosan nano/microformulations for antimicrobial protection of leather with a potential impact in tanning industry, *Materials* **15**, 1750, 2022.
12. Ma, J., Duan, L., Lu, J., et al.; Fabrication of modified hydrogenated castor oil/GPTMS-ZnO composites and effect on UV resistance of leather, *Scientific Reports* **7**, 3742, 2017.
13. P Bhasi, A., Hanna Wilson, N. and Palanisamy, T.; Nanosized hexagonal boron nitride and polyethylene glycol-filled leathers for applications demanding high thermal insulation and impact resistance, *ACS omega* **7**, 45120-45128, 2022.
14. Elsayed, H., Hasanin, M. and Rehan, M.; Enhancement of multifunctional properties of leather surface decorated with silver nanoparticles (Ag NPs), *Journal of Molecular Structure* **1234**, 130130, 2021.
15. Pan, F., Xiao, Y., Zhang, L., et al.; Leather wastes into high-value chemicals: Keratin-based retanning agents via UV-initiated polymerization, *Journal of Cleaner Production* **383**, 135492, 2023.
16. Kumar, P., Bohidar, H.; Aqueous dispersion stability of multi-carbon nanoparticles in anionic, cationic, neutral, bile salt and pulmonary surfactant solutions, *Colloids and Surfaces A-Physicochemical and Engineering Aspects* **361**, 13-24, 2010.
17. Madshal, M. A., Abdelghany, A. M., Abdelghany, M. I., et al.; Biocompatible borate glasses doped with Gd_2O_3 for biomedical applications, *The European Physical Journal Plus* **137**, 1014, 2022.
18. Ning, G. Q., Zhou, J. B., Liao, X. P., et al.; Synthesis of a waterborne melamine resin and its retanning behaviors investigation, *JALCA* **117**, 288-295, 2022.
19. Naresh, G., Borah, J., Borgohain, C., et al.; Synthesis, characterization and effect of dopant on magnetic hyperthermic efficacy of gd2o3 nanoparticles, *Materials Research Express* **8**, 115014, 2021.
20. Peng, L. Q., Guo, L. J., Li, J. H., et al.; Rapid and highly selective removal of cesium by prussian blue analog anchored on porous collagen fibers, *Separation and Purification Technology* **307**, 122858, 2023.
21. Sun, N., Zhou, J. b., Liao, X. P., et al.; Synthesis and retanning performance of a novel melamine resin with ultralow formaldehyde content, *JALCA* **118**, 23-35, 2023.
22. Zhang, L., Chen, Y., Zhao, M., et al.; Efficient adsorption of uranyl ions from aqueous solution by Gd_2O_3 and Gd_2O_3–MgO composite materials, *International Journal of Environmental Science and Technology* **20**, 815-830, 2023.
23. Ding, W., Liu, H., Pang, X. Y., et al.; Engineering a pioneering melamine resin based on saccharide-derived aldehyde: Structure characterization and application for eco-leather production, *Industrial Crops and Products* **185**, 115133, 2022.
24. Tang, Y., Li, M. F., Zhou, J. B., et al.; Polyethyleneimine/hydrated titanium oxide-functionalized fibrous adsorbent for removing cobalt: Adsorption performance and irradiation stability, *Environmental Research* **211**, 112916, 2022.
25. Wang, G., Li, Y., Wang, E., et al.; Experimental study on preparation of nanoparticle-surfactant nanofluids and their effects on coal surface wettability, *International Journal of Mining Science and Technology* **32**, 387-397, 2022.
26. Hou, J., Du, W., Meng, F., et al.; Effective dispersion of multi-walled carbon nanotubes in aqueous solution using an ionic-gemini dispersant, *Journal of Colloid and Interface Science* **512**, 750-757, 2018.
27. Wang, X., Sun, S., Zhu, X., et al.; Application of amphoteric polymers in the process of leather post-tanning, *Journal of Leather Science and Engineering* **3**, 9, 2021.
28. Yi, Y., Zhang, Y., Mansel, B., et al.; Effect of dialdehyde carboxymethyl cellulose cross-linking on the porous structure of the collagen matrix, *Biomacromolecules* **23**, 1723-1732, 2022.
29. He, X., Huang, Y., Xiao, H., et al.; Tanning agent free leather making enabled by the dispersity of collagen fibers combined with superhydrophobic coating, *Green Chemistry* **23**, 3581-3587, 2021.
30. Li, Q., Yi, Y., Wang, Y.-n., et al.; Effect of cationic monomer structure on the aggregation behavior of amphoteric acrylic polymer around isoelectric point, *Journal of Leather Science and Engineering* **4**, 4, 2022.
31. Liu, Z., Zou, Y., Zhang, Q., et al.; Distinct binding dynamics, sites and interactions of fullerene and fullerenols with amyloid-β peptides revealed by molecular dynamics simulations, *International Journal of Molecular Sciences* **20**, 2048, 2019.